Proceedings of IMECE04
2004 ASME International Mechanical Engineering Congress and Exposition
November 13-20, 2004, Anaheim, California USA

IMECE2004-59990

MODELING OF PNEUMATIC ACTUATOR SYSTEM FOR HIGH PERFORMANCE NONLINEAR CONTROLLER DESIGN

Meihua Tai*
Robotics and Intelligent Systems Laboratory (RISL)
Department of Mechanical Engineering
Polytechnic University
Six MetroTech Center
Brooklyn, NY 11201
Email: mtai@duke.poly.edu
WWW: http://risl.poly.edu

Ke Xu
Second Coauthor
Robotics and Intelligent Systems Laboratory (RISL)
Department of Mechanical Engineering
Polytechnic University
Six MetroTech Center
Brooklyn, NY 11201
Email: kxu01@utopia.poly.edu
WWW: http://risl.poly.edu

ABSTRACT

Modern applications in robotics such as teleoperations and haptics require high performance force actuators. Pneumatic actuators have significant advantages over electrical motors in terms of force-to-mass ratio. However, position and force control of these actuators in applications that require high bandwidth is not trivial because of the compressibility of air and highly nonlinear flow through pneumatic system components. In this paper, we develop a detailed model of a pneumatic actuator system comprised of a double acting cylinder and a proportional servo valve to be used in position, force or hybrid position and force control.

NOMENCLATURE

R Ideal gas constant
C_v Specific heat at constant volume
C_p Specific heat at constant pressure
k Specific heat ratio
P Pressure of gas
V Volume of gas
ρ Density of gas
T Temperature of gas
$\dot{m}$ Mass flow rate
$\dot{m}_{en}$ Mass flow rate entering to the controlled volume of gas
$\dot{m}_{ex}$ Mass flow rate exiting from the controlled volume of gas
$\dot{Q}$ Heat transfer rate to the controlled volume of gas
h_{en} Enthalpy of the gas entering to the controlled volume of gas
h_{ex} Enthalpy of the gas exiting from the controlled volume of gas
v_{en} Velocity of the gas entering to the controlled volume of gas
v_{ex} Velocity of the gas exiting from the controlled volume of gas
E Total energy of the controlled volume of gas
U Internal energy of control volume of gas
W Work delivered by the controlled volume of gas to the environment
P_{ca}, P_{cb} Static pressure of chamber A and chamber B of the cylinder
A_a, A_b Effective area of piston at chamber A and B of the cylinder
T_a, T_b Static temperature of chamber A and chamber B of the cylinder
P_a Pressure of the ambient air
P_u Upstream static pressure
P_d Downstream static pressure
P_s Pressure in the reservoir tank
T_s Temperature in the reservoir tank

*Corresponding author.

INTRODUCTION

Modern existing and emerging new applications in robotics require high performance force actuators or hybrid force and position actuators with high force output per unit weight. Compared to traditional geared electrical motors and hydraulic actuators, pneumatic actuators have several advantages [1] in these applications beside their being low cost and clean-operation. Pneumatic actuators can also provide static high force output for a long duration without additional cooling systems as in the case of direct drive electrical motors.

However, position and force control of these actuators in applications that require high bandwidth is difficult because of the compressibility of air and the highly nonlinear flow through pneumatic system components. Due to these difficulties, early use of pneumatic actuators had been limited to simple applications that require only positioning at the two ends of the piston stroke. With the increasingly in-depth understanding of the thermodynamics and flow characteristics [2], linear position controllers have been developed [3, 4] around the operating point of the mid-stroke. More recently, nonlinear control laws for force control have been developed using feedback linearization techniques [5, 6], or Lyapunov stability arguments [7].

To study the control aspects of pneumatic actuators for applications in precision position control, force control and hybrid position and force control, we developed a simple pneumatic testbed that consists of a double acting cylinder with rods and proportional servo valve connected by tubes. In this paper, we derive a detailed model of the pneumatic actuator system.

BACKGROUND

In this section, we briefly introduce some background knowledge on basic pneumatics, mainly on the dynamics of a controlled volume of gas and on the steady flow of an ideal gas through a cross section.

Dynamics of a Controlled Volume of Gas

Consider a controlled volume of gas which is charged from a reservoir and discharged to an ambient air. We assume that the gas is perfect, and the pressure and temperature of the controlled volume are homogeneous.

For a controlled volume of gas, the energy equation from the first law of thermodynamics can be written as

$$\dot{Q} + \dot{m}_{en}\left(h_{en} + \frac{v_{en}^2}{2}\right) - \dot{m}_{ex}\left(h_{ex} + \frac{v_{ex}^2}{2}\right) = \dot{E} + \dot{W}. \quad (1)$$

The gas entering to the chamber comes from a reservoir. Since the gas in the reservoir has zero velocity, its enthalpy is represented by the stagnation enthalpy h_0,

$$h_{en} + \frac{v_{en}^2}{2} = h_0 = C_p T_0, \quad (2)$$

where T_0 is the temperature of the gas in the reservoir. Similarly, since the velocity of the gas of the controlled volume is very small compared to the exiting velocity v_{ex}, the enthalpy of the exiting gas is represented by that of the controlled volume,

$$h_{ex} + \frac{v_{ex}^2}{2} = h = C_p T., \quad (3)$$

where T is the temperature of the controlled volume.

The total energy of the gas consists of three components: the kinetic energy, the potential energy and the internal energy. The rate of change in kinetic and potential energies of the controlled volume are assumed small in comparison to the rate of change of the corresponding internal energy and are therefore ignored. For an ideal gas, the internal energy is given by

$$U = C_v \rho V T. \quad (4)$$

Using the ideal gas law,

$$P = \rho R T, \quad (5)$$

the internal energy can be rewritten as

$$U = \left(\frac{C_v}{R}\right) PV. \quad (6)$$

So, the rate of change of the total energy of the control volume is

$$\dot{E} = \dot{U} = \frac{C_v}{R}\frac{d}{dt}(PV) = \frac{C_v}{R}(\dot{P}V + P\dot{V}). \quad (7)$$

The rate of the work done by the controlled volume of gas to the environment is

$$\dot{W} = P\dot{V}. \quad (8)$$

By substituting Eqs. (2), (3), (7) and (8) into Eq. (1), we have

$$\dot{Q} + C_p(\dot{m}_{en}T_0 - \dot{m}_{ex}T) = \frac{C_v}{R}\dot{P}V + \left(\frac{C_v}{R} + 1\right)P\dot{V}. \quad (9)$$

From the relationships among the three constants, C_v, C_p and R,

$$\begin{aligned} C_p &= C_v + R, \text{ and} \\ k &= \frac{C_p}{C_v}, \end{aligned} \tag{10}$$

we have

$$\begin{aligned} \frac{C_v}{R} &= \frac{1}{k-1}, \text{ and} \\ C_p &= \frac{k}{k-1}R. \end{aligned} \tag{11}$$

By substituting Eq. (11) into Eq. (9), the energy equation can alternatively be expressed as

$$\dot{Q} + \frac{k}{k-1}R(\dot{m}_{en}T_0 - \dot{m}_{ex}T) = \frac{1}{k-1}\dot{P}V + \frac{k}{k-1}P\dot{V}. \tag{12}$$

Eq. (12) states how the pressure of the controlled volume of gas varies as a function of the entering and exiting flow rates which, in practical pneumatic systems, are usually regulated by the servo valves.

As in Richer and Hurmuzlu [1], we take into account different thermal characteristics of charging and discharging processes of the controlled volume. It is experimentally found [8] that the temperature of the controlled volume lays between the theoretical adiabatic and isothermal curves. When, the controlled volume is being charged, the temperature is closer to the adiabatic curve; and when the controlled volume is being discharged, the process is closer to the isothermal situation.

If the process is considered to be adiabatic, i.e., $\dot{Q} = 0$, then from Eq. (12), the rate of change of the pressure is

$$\dot{P} = \frac{RT}{V}(k\dot{m}_{en}\frac{T_0}{T} - k\dot{m}_{ex}) - k\frac{P}{V}\dot{V}. \tag{13}$$

If the process is considered to be isothermal, i.e., $T = T_0 =$ constant, the rate of change of the total energy is

$$\dot{E} = \dot{U} = C_v\dot{m}T = C_v(\dot{m}_{en} - \dot{m}_{ex})T. \tag{14}$$

Then from Eqs. (7) and (14), we have

$$\dot{P} = \frac{RT}{V}(\dot{m}_{en} - \dot{m}_{ex}) - \frac{P}{V}\dot{V}. \tag{15}$$

By comparing Eqs. (13) and (15), the dynamics of the controlled volume can be described as

$$\dot{P} = \frac{RT}{V}(k_{en}\dot{m}_{en} - k_{ex}\dot{m}_{ex}) - k_w\frac{P}{V}\dot{V}, \tag{16}$$

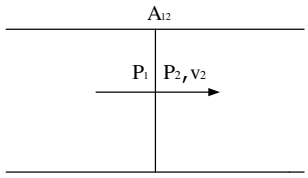

Figure 1. Flow passage

where $k_{en} \in [1, \frac{kT_0}{T}]$, $k_{ex} \in [1,k]$ and $k_w \in [1,k]$, depending on the actual heat transfer characteristics during the process.

Steady Flow of an Ideal Gas

Consider a compressible fluid passing through a duct as shown in Fig. 1. At some section A_{12} where the velocity is uniform across the section and the static pressure is P_2, the flow rate of the fluid is given by

$$\dot{m} = \rho_2 A_{12} v_2, \tag{17}$$

where ρ_2 is the static density, A_{12} is the area of the cross section and v_2 is the velocity.

In this study, we define the total pressure as the pressure at the local isentropic stagnation state. This is the hypothetical state reached at any point in a flowing gas by isentropically slowing the gas to zero velocity. Then, the total pressure is given by [9],

$$\frac{P_1}{P_2} = \left(1 - \frac{k-1}{2kRT_1}v_2^2\right)^{\frac{k}{1-k}}, \tag{18}$$

where P_1 and T_1 are the total pressure and temperature. The isentropic process relating P_1 and P_2 determines the relationship between density and pressure as

$$\frac{\rho_2}{\rho_1} = \left(\frac{P_2}{P_1}\right)^{\frac{1}{k}}, \tag{19}$$

and the relationship between temperature and pressure as

$$\frac{T_2}{T_1} = \left(\frac{P_2}{P_1}\right)^{\frac{k-1}{k}}. \tag{20}$$

From the ideal gas law given by Eq. (5) and the relationship between density and pressure given by Eq. (19), we have

$$\rho_2 = \frac{P_1}{RT_1}\left(\frac{P_2}{P_1}\right)^{\frac{1}{k}}. \tag{21}$$

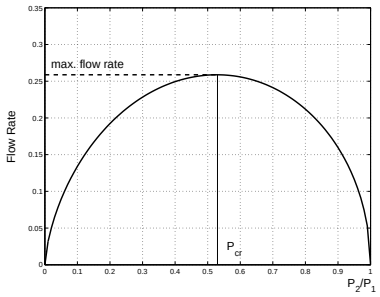

Figure 2. Flow rate as a function of pressure ratio

From Eq. (18), the local velocity can be obtained as

$$v_2 = \sqrt{\frac{2kRT_1}{k-1}\left[1-\left(\frac{P_2}{P_1}\right)^{\frac{k-1}{k}}\right]}. \tag{22}$$

Then, from Eqs. (17), (21) and (22), the flow rate can be rewritten as

$$\dot{m} = \frac{A_{12}P_1}{\sqrt{T_1}}\sqrt{\frac{2k}{(k-1)R}\left[\left(\frac{P_2}{P_1}\right)^{\frac{2}{k}}-\left(\frac{P_2}{P_1}\right)^{\frac{k+1}{k}}\right]}. \tag{23}$$

Equation (23) is strictly valid at any point in a flowing gas. It shows that if the total pressure and temperature and the cross section area are constants, the flow rate is a function of the ratio of the static pressure to the total pressure, $\frac{P_2}{P_1}$, as shown in Fig. 2.

The critical pressure ratio, P_{cr}, at which the maximum flow rate is achieved can be obtained by setting the derivative of Eq. (23) equal to zero. It is

$$P_{cr} = \left(\frac{2}{k+1}\right)^{\frac{k}{k-1}}, \tag{24}$$

and the maximum flow rate at this critical pressure ratio is

$$\dot{m}_{max} = \frac{A_{12}P_1}{\sqrt{T_1}}\sqrt{\frac{k}{R}\left(\frac{2}{k+1}\right)^{\frac{k+1}{k-1}}}. \tag{25}$$

MODELING

The basic components of a typical pneumatic actuator consists of chambers, servo valves, connecting tubes and necessary sensors to measure position, chamber pressure and force. To study the control aspects of pneumatic actuators for applications

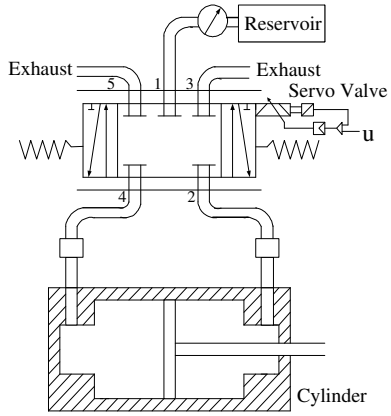

Figure 3. Schematic diagram of a pneumatic actuator system for position and/or force control

in precision position control, force control and hybrid position and force control, we developed a simple pneumatic testbed. The schematic diagram of the system is as shown in Fig. 3. The systems consists of one double acting pneumatic actuator, one 5 port 3 way proportional servo valve, two tubes connecting each chamber of the actuator to the valve, two pressure sensors to measure the chamber pressure and one range sensor to measure the position of the piston. For the force control applications, there will be additional force sensors installed.

Actuator

For the double acting pneumatic actuator, the piston and rod carry external weight for positioning and they bear external forces coming from the interaction with the environment. The force that moves the piston-rod-load and that counteracts the external forces are produced by the regulation of the pressure of the two chambers of the cylinder. The dynamics of the pressure of each chamber is governed by Eq. (16). The the origin of the piston displacement, x_p, be at the mid stroke of the piston. Then,

$$\begin{aligned}\dot{P}_{ca} &= \frac{RT_a}{V_a}(k_{en1}\dot{m}_{en1}-k_{ex1}\dot{m}_{ex1})-k_{w1}\frac{P_{ca}}{V_a}\dot{V}_a \\ &= \frac{RT_a}{V_{a0}+A_a(\frac{L}{2}+x_p)}(k_{en1}\dot{m}_{en1}-k_{ex1}\dot{m}_{ex1}) \\ &\quad -k_{w1}\frac{P_{ca}}{V_{a0}+A_a(\frac{L}{2}+x_p)}A_a\dot{x}_p\end{aligned} \tag{26}$$

is the equation for the dynamics of the pressure for chamber A where V_{a0} is the inactive volume at the end of stroke of chamber A and admission ports, and L is the piston stroke. The equation

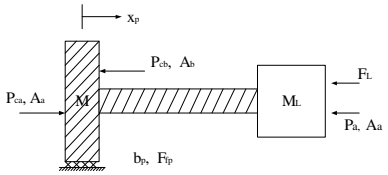

Figure 4. Schematic diagram of piston-rod-load assembly

for the dynamics of the pressure of chamber B is

$$\begin{aligned}\dot{P}_{cb} &= \frac{RT_b}{V_b}(k_{en2}\dot{m}_{en2} - k_{ex2}\dot{m}_{ex2}) - k_{w2}\frac{P_{cb}}{V_b}\dot{V}_b \\ &= \frac{RT_b}{V_{b0} + A_b(\frac{L}{2} - x_p)}(k_{en2}\dot{m}_{en2} - k_{ex2}\dot{m}_{ex2}) \\ &\quad + k_{w2}\frac{P_{cb}}{V_{b0} + A_b(\frac{L}{2} - x_p)}A_b\dot{x}_p\end{aligned} \tag{27}$$

where V_{b0} is the inactive volume at the end of stroke of chamber B and admission ports.

When chamber A is being charged, chamber B is being discharged. Therefore, $\dot{m}_{en1} > 0$, $\dot{m}_{ex1} = 0$, $\dot{m}_{en2} = 0$ and $\dot{m}_{ex2} > 0$. Similarly, when chamber B is being charged, chamber A is being discharged. Therefore, $\dot{m}_{en1} = 0$, $\dot{m}_{ex1} > 0$, $\dot{m}_{en2} > 0$ and $\dot{m}_{ex2} = 0$.

Figure 4 shows the schematic diagram of the piston-rod-load system. The equations of motion for the piston-rod-load assembly can be obtained from the Newton's Second law as

$$(M + M_L)\ddot{x}_p + b_p\dot{x}_p + F_{fp} + F_L = P_{ca}A_a - P_{cb}A_b - P_aA_r \tag{28}$$

where M is the mass for of the piston and rod, M_L is the mass of the external load, b_p and F_{fp} are the viscous damping coefficient and the Coulomb friction between the piston and the cylinder wall, F_L is the external force acting on the piston, P_a is the ambient air pressure and A_r is the cross section area of the rod.

Flow Through an Orifice

The geometry of an orifice affects the flow rate through it in a very complicated way since it directly influences the characteristics of the flow process. The flow rate equation (23) is strictly correct provided that the total pressure, total temperature and static pressure are known at some area in the restriction across which the velocity is constant. However, none of these quantities are practically measurable. In practices, we would like to relate the flow rate through a nozzle, an orifice or a valve to upstream and downstream states such as pressure and temperature.

For a valve charging a chamber from a reservoir, the flow process from a point in the reservoir tank to the exit of the valve may be considered isentropic if the orifice area decreases monotonically. In this case, since there is no energy lost, the total pressure and temperature at the exit section equal the total pressure and temperature in the tank. Furthermore, if the tank is large enough for the velocity approaching the valve to be small, the static pressure in the tank is virtually the same as the total pressure. Then, the upstream (tank) static pressure, P_u, can be taken as the total pressure at the exit section, P_1 in Eq. (23).

It is not usually convenient to measure static pressure at the exit section of the orifice. If the orifice discharges to the atmosphere, the exit static pressure will be equal to atmospheric pressure provided that this is not lower than the critical pressure corresponding to the total pressure in the tank. If the ambient pressure is less than the critical pressure, the pressure at the exit (presumed to be the minimum nozzle area) will be exactly critical and the gas will continue to expand after it leaves the nozzle. This is called *sonic* or *choked* condition. Thus the curve of nozzle flow vs. pressure ratio will follow the dashed line in Fig. 2.

If the nozzle is in a line, the static pressure at the throat will not necessarily equal down stream static pressure. The reason is simply that as the gas slows down after leaving the nozzle, some of the kinetic energy is usually converted into pressure. The percentage of recovery of the dynamic pressure at the throat depends on the geometric design of the exit section of the nozzle. Usually if the downstream area increases abruptly at the exit section, it can be assumed that all of the dynamic pressure is lost in the expansion process. If the orifice has abrupt area change at the entrance section, the flow separates from the orifice wall and forms its own nozzle after passing into or through the inlet section. The minimum-area cross section area is thought of as the effective area of the orifice.

To make the problem mathematically tractable for controller designs, we make the following assumptions for the flow through a valve.

Assumption 1. *The P_1 in Eq. (23) is equal to the upstream static pressure if the approaching gas velocity is small.*

Assumption 2. *The T_1 in Eq. (23) is equal to the upstream static or total temperature, T_u, since the difference between them is even less than the difference between static and total pressures.*

Assumption 3. *The P_2 in Eq. (23) equal the downstream static pressure, P_d, if recovery is negligible.*

Assumption 4. *The A_{12} in Eq. (23) equal to the effective area rather than the geometric or physical minimum orifice area. We represent the effective area by C_fA_{12} where C_f is called a discharge coefficient.*

Assumption 5. *The correction term for the mass flow rate due to the reduction of the average velocity at the exit than the isentropic value is lumped with the discharge coefficient, C_f.*

Assuming that all the provisions of the assumptions 1-5 holds, in the following we take $P_1 = P_u$ and $P_2 = P_d$. We also assume that the gas is adiabatic everywhere in the valve and the flow is isentropic everywhere except across normal shock wave.

During charging and discharging process, the pressure drop across the valve orifice is usually large and the flow has to be treated as compressible and turbulent; and the flow characteristics changes dramatically depends on the ratio of the upstream pressure and the downstream pressure. When $\frac{P_d}{P_u} = 1$, the downstream pressure is the same as the upstream pressure and there is no flow through the orifice. When the downstream to upstream pressure ratio is greater than a critical value P_{cr} but less than 1, the flow is subsonic at the exit plane. As the difference between the upstream pressure and the downstream pressure increases, the stream velocity at the throat increases till to the point where the flow reaches its critical regime. At this point, the velocity of the gas in the throat is equal to the speed of sound calculated at the throat and would never get larger even if the pressure difference increases. Further reducing the downstream pressure will not affect the flow state at the throat because the flow is choked in the valve. In this regime, the pressure of the jet leaving the nozzle is greater than the downstream pressure but stays constant, $P_{cr}P_u$. The sudden reduction in the pressure causes the jet to expand in an explosive fashion. This situation is quite common and occurs when there is little load on the piston and when the downstream pressure is much smaller than the upstream pressure.

In this study, we ignore the effect of the connecting tubes on the pressure and time delays. Therefore, when the chamber is being charged from a reservoir, the upstream pressure is the same as the reservoir pressure and the downstream pressure is the same as the chamber pressure; and when the chamber is being discharged to the ambient air, the upstream pressure is the same as the chamber pressure and the downstream pressure is the same as the ambient air pressure.

In summary, when the chamber is being charged from the reservoir, the flow rate is

$$\dot{m}_{eni} = \begin{cases} C_f \frac{A_{v_{en}} P_s}{\sqrt{T_s}} \sqrt{\frac{2k}{(k-1)R}\left[\left(\frac{P_{ci}}{P_s}\right)^{\frac{2}{k}} - \left(\frac{P_{ci}}{P_s}\right)^{\frac{k+1}{k}}\right]} & \text{if } \frac{P_{ci}}{P_s} \geq P_{cr} \\ C_f \frac{A_{v_{en}} P_s}{\sqrt{T_s}} \sqrt{\frac{k}{R}\left(\frac{2}{k+1}\right)^{\frac{k+1}{k-1}}} & \text{if } \frac{P_{ci}}{P_s} < P_{cr} \end{cases}, \tag{29}$$

and when the chamber is being discharged to the ambient air, the flow rate is

$$\dot{m}_{exi} = \begin{cases} C_f \frac{A_{v_{ex}} P_{ci}}{\sqrt{T_i}} \sqrt{\frac{2k}{(k-1)R}\left[\left(\frac{P_a}{P_{ci}}\right)^{\frac{2}{k}} - \left(\frac{P_a}{P_{ci}}\right)^{\frac{k+1}{k}}\right]} & \text{if } \frac{P_a}{P_{ci}} \geq P_{cr} \\ C_f \frac{A_{v_{ex}} P_{ci}}{\sqrt{T_i}} \sqrt{\frac{k}{R}\left(\frac{2}{k+1}\right)^{\frac{k+1}{k-1}}} & \text{if } \frac{P_a}{P_{ci}} < P_{cr} \end{cases}, \tag{30}$$

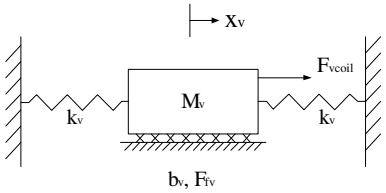

Figure 5. Schematic diagram of spool dynamics

where $i = a$ for chamber A and $i = b$ for chamber B, $A_{v_{en}}$ is the valve area for input path and $A_{v_{ex}}$ is the valve area for the exhaust path.

Proportional Servo Valve Model

The valve areas, $A_{v_{en}}$ and $A_{v_{ex}}$ are regulated by the movement of the valve spool which is commanded by the voice coil. Figure 5 shows the schematic diagram of the spool inside the valve. The equation of motion of the spool can be obtained from the Newton's Second Law as

$$M_v\ddot{x}_v + b_v\dot{x}_v + 2k_v x_v + F_{fv} = F_{vcoil}, \tag{31}$$

where x_v is the displacement of the spool, M_v is the mass of the spool, b_v and K_v are the viscous damping coefficient and spring constant of the spool valve respectively, F_{fv} is the Coulomb friction, and F_{vcoil} is the force generated by the voice coil. For the proportional servo valve we used, F_{vcoil} is proportional to the voltage command signal u, that is,

$$F_{vcoil} = k_u u, \tag{32}$$

where k_u is a know constant.

As the spool position varies, it regulates the opening and closing areas of the each port. From the geometry, we can obtain the valve areas, $A_{v_{en}}$ and $A_{v_{ex}}$, as functions of the spool displacement, x_v, as [1]

$$A_{v_{en}}(x_v) = \begin{cases} 0 & \text{if } x_v < p_w - R_h \\ n_h\left[2R_h^2 \arctan\left(\sqrt{\frac{R_h - p_w + x_v}{R_h + p_w - x_v}}\right) - (p_w - x_v)\sqrt{R_h^2 - (p_w - x_v)^2}\right] & \text{if } p_w - R_h < x_v < p_w + R_h \\ n_h\pi R_h^2 & \text{if } x_v \geq p_w + R_h \end{cases} \tag{33}$$

and

$$A_{v_{ex}}(x_v) = \begin{cases} n_h \pi R_h^2 \\ \qquad \text{if} \quad x_v < -p_w - R_h \\ n_h \left[2R_h^2 \arctan\left(\sqrt{\frac{R_h - p_w + |x_v|}{R_h + p_w - |x_v|}} \right) \right. \\ \qquad \left. -(p_w - |x_v|)\sqrt{R_h^2 - (p_w - |x_v|)^2} \right] \\ \qquad \text{if} \quad -p_w - R_h < x_v < -p_w + R_h \\ 0 \\ \qquad \text{if} \quad x_v \geq -p_w + R_h \end{cases} \tag{34}$$

where p_w is the half of the spool width, R_h is the radius of hole, and n_h is the number of active holes for an air path in the sleeve.

These are very complicated non-analytic functions. For advanced nonlinear controller design, it is required these functions to be analytic. We therefore, approximated $A_{v_{en}}$ with

$$\bar{A}_{v_{en}} = n_h \pi R_h^2 \left(1 + \frac{e^{a_{en}(t-p_w)} - e^{-a_{en}(t-p_w)}}{e^{a_{en}(t-p_w)} + e^{-a_{en}(t-p_w)}} \right), \tag{35}$$

where

$$a_{en} = \frac{1}{2n_h \pi R_h^2} \frac{dA_{v_{en}}(x_v)}{dx_v}\bigg|_{x_v = p_w}, \tag{36}$$

and $A_{v_{ex}}$ with

$$\bar{A}_{v_{ex}} = n_h \pi R_h^2 \left(1 + \frac{e^{-a_{ex}(t+p_w)} - e^{a_{ex}(t+p_w)}}{e^{a_{ex}(t+p_w)} + e^{-a_{ex}(t+p_w)}} \right), \tag{37}$$

where

$$a_{ex} = \frac{1}{2n_h \pi R_h^2} \frac{dA_{v_{ex}}(x_v)}{dx_v}\bigg|_{x_v = -p_w}. \tag{38}$$

Figure 6 shows the valve areas and their approximations as functions of valve spool displacement.

In summary, Eqs.(28), (26), (27), (29), (30), (35), (37) and (31) completely describe the dynamics of the pneumatic actuator system.

CONCLUSION

In this paper, we presented a detailed component-wide model of a pneumatic actuator system that comprises of a double acting cylinder, a proportional servo valve, two connecting tubes and necessary sensors.

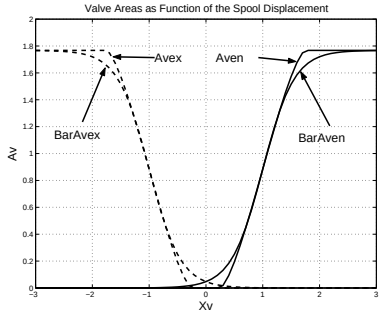

Figure 6. Valve areas and their approximations as functions of valve spool displacement

REFERENCES

[1] Edmond Richer and Yildirim Hurmuzlu. A high performance pneumatic force actuator system part 1 - nonliner mathematical model. *ASME Journal of Dynamic Systems, Measurement, and Control*, 122(3):416–425, 2000.

[2] J. E. Shearer. Study of pneumatic process in the continuous control of motion with compressed air-i, ii. *Transactions of ASME*, 1956.

[3] C. R. Burrow and C. R. Webb. Use of the root loci in design of pneumatic servo-motors. *Control*, 1966.

[4] S. Liu and J. E. Bobrow. An analysis of a pneumatic servo system and its application to a computer-controlled robot. *Journal of Dynamic Systems, Measurement, and Control*, 110, 1988.

[5] A. Bouhal, E. Richard, and S. Scarvarda. An experimental comparative study of linear and nonlinear adaptive pressure regulation. In *Proceedings of the 6th International Fluid Power Workshop on Modeling and Simulation*, pages 225–238, 1993.

[6] T. Kimura, S. Hara, T. Fujita, and T. Kagawa. Control for pneumatic actuator systems using feedback linearization with disturbance rejection. In *Proceedings of 1995 American Control Conference*, pages 825–829, Seattle, WA, June 1995.

[7] S. Kawmura, K. Miyata, H. Hanafusa, and K. Isisa. PI type hierachical control scheme for pneumatic robots. In *Proceedings of 1989 International Conference on Robotics and Automation*, pages 1953–1958, Scottsdale, AZ, 1989.

[8] A. M. Al-Ibrahim and D. R. Otis. Transient air temperature and pressure measurements during the charging and discharging processes of an actuating pneumatic cylinder. In *Proceedings of the 45th National Conference on Fluid Power*, 1992.

[9] B. W. Andersen. *The Analysis and Design of Pneumatic Systems*. Krieger Publishing Company, 2001.